Biocatalysis and Agricultural Biotechnology 22 (2019) 101373

Contents lists available at ScienceDirect

Biocatalysis and Agricultural Biotechnology

journal homepage: http://www.elsevier.com/locate/bab

Biologically synthesized silver nanoparticles against pathogenic bacteria: Synthesis, calcination and characterization

K. Mathivanan [a,*], R. Selva [a], J. Uthaya Chandirika [a], R.K. Govindarajan [b], R. Srinivasan [c], G. Annadurai [a,**], Pham Anh Duc [d]

[a] Environmental Nanotechnology Division, Sri Paramakalyani Centre of Excellence in Environmental Sciences, Manonmaniam Sundaranar University, Alwarkurichi, Tamil Nadu, 627 412, India
[b] Department of Zoology, School of Life Sciences, Periyar University, Salem, 636011, Tamil Nadu, India
[c] Department of Oceanography and Coastal Area Studies, School of Marine Sciences, Alagappa University, 623409, Tamil Nadu, India
[d] Faculty of Environment and Labour Safety, Ton Duc Thang University, Ho Chi Minh City, Viet Nam

ARTICLE INFO

Keywords:
Bacteria
AgNPs
Calcination
Diffusion assay
Antibacterial activity

ABSTRACT

In this study, the silver nanoparticles (AgNPs) were synthesized using a strain *Bacillus subtilis* KMS2-2 by extracellularly. The effect of calcination (200 °C for 30 min) on structural characteristics and antibacterial activity of the AgNPs were investigated. The inhibitory effect of AgNPs against pathogenic bacteria such as *Pseudomonas fluorescens* MTCC 1749, *Proteus mirabilis* MTCC 425, *Escherichia coli* MTCC 1610, *Bacillus cereus* and *Staphylococcus aureus* MTCC 2940 was tested by agar-well diffusion method. The synthesized AgNPs before and after calcination were spherical crystalline in nature and had size range from 18–100 nm and 49–153 nm, respectively and were determined by scanning electron microscope (SEM) and X-ray diffraction analysis (XRD). Further, Fourier transform Infrared spectroscopic (FT-IR) analysis revealed the presence of bioactive compounds in the crude AgNPs as capping materials. The *in vitro* antibacterial studies revealed that crude AgNPS strongly inhibited the growth of tested pathogenic bacteria, whereas, the calcined AgNPs didn't show growth inhibition activity.

1. Introduction

Evolving multi drug resistant microbes are the most important threats to public health and there is urgent need to explore novel antimicrobial agents (Boovaragamoorthy et al., 2019; Saravanan et al., 2018c; Van Duin and Paterson, 2016). Due to increased attention on emergence of multidrug resistance in microbes, the biomedical and pharmaceutical sector is initiating to screen the active compounds against it. Several decades ago, silver and its salts have been used as antimicrobial agents in primary health and wound care (Munteanu et al., 2016; Pugazhendhi et al., 2018c; Saratale et al., 2017; Saravanan et al., 2018b; Shanmuganathan et al., 2018). However, the usage of silver was drastically reduced due to emergence and development of new antibiotics (Deljou and Goudarzi, 2016). There has been growing interest of nanotechnology in recent years, the application of nanoparticles in various fields are developed. The nanoparticles have optical, electronic, magnetic, and catalytic properties in terms of their size, shape and chemical surrounding (Fathima et al., 2018; Jiang et al., 2019; Pugazhendhi et al., 2018b, 2019; Vasantharaj et al., 2019). Nanoparticles are widely used in different fields such as industries (food packing, paint, paper, leather and textile) (Jacob et al., 2018; Saratale et al., 2018a; Sathiyavimal et al., 2018), nano-fertilizer in agriculture, wastewater treatment and medicine etc. (Hussein et al., 2019; Jishma et al., 2018; Premkumar et al., 2018). Also, the nanoparticles are extensively used in renewable energy (Kumar et al., 2019; Pugazhendhi et al., 2018d) electronic devices due to their high conductivity and stability (Kumar et al., 2018; Murphin Kumar et al., 2017).

The nanoparticles can be synthesized by diverse methods including physical, chemical and hybrid systems. However, the nanoparticle synthesis by these methods is expensive and produces undesirable and

* Corresponding author.
** Corresponding author.
E-mail addresses: kritamathi@gmail.com (K. Mathivanan), selvajeni1993@gmail.com (R. Selva), chandirikajram@gmail.com (J.U. Chandirika), biogovindarajan@gmail.com (R.K. Govindarajan), sandalsrini@gmail.com (R. Srinivasan), gannadurai@msuniv.ac.in (G. Annadurai), phamanhduc@tdtu.edu.vn (P.A. Duc).

https://doi.org/10.1016/j.bcab.2019.101373
Received 2 September 2019; Received in revised form 30 September 2019; Accepted 4 October 2019
Available online 4 October 2019

toxic byproducts that are hazard to environment (Patra and Baek, 2014). The synthesis of nanoparticles by biological method has received profound interest because of its effectiveness, less cost and ecofriendly nature (Oves et al., 2018; Saravanan et al., 2018a). It has been previously reported that biological sources (bacteria, algae, fungi, yeast and various parts of plants) and their derivatives effectively synthesized the nanoparticles (Arya et al., 2019; Mahmoud et al., 2016; Ramkumar et al., 2017; Saratale et al., 2018b; Soliman et al., 2018). The synthesis of metal nanoparticles by microbes can accomplish either intracellularly or extracellularly. Comparison with extracellular process, the intracellular process requires more steps to recover the synthesized nanoparticles (Kalimuthu et al., 2008). In particular, the extracellular synthesis of AgNPs has significant advantage in biomedical and pharmaceutical sector due to their extensive usage as antimicrobial, anticancer and anti-inflammatory agents (Kathiravan et al., 2014; Pugazhendhi et al., 2018a; Shanmuganathan et al., 2019a; Wong et al., 2009). Additionally, the larvicidal and nematicidal properties of biologically synthesized AgNPs have been experimentally proven (Banu and Balasubramanian, 2015; Mahmoud et al., 2016).

Various species of bacteria have been successfully studied for diverse metal nanoparticles synthesis, especially, in AgNPs (Deljou and Goudarzi, 2016; Mahmoud et al., 2016; Paul and Sinha, 2014; Thomas et al., 2014). Particularly, the Gram positive genera of *Bacillus* are widely used in the pharmaceutical, food and dairy industry due to its potential active compounds production as well as in nanoparticle synthesis (Deljou and Goudarzi, 2016). The present study aimed to synthesize the AgNPs by culture supernatant of Gram positive bacterial strain, *Bacillus subtilis* KMS2-2 and to examine the calcination temperature (200 °C for 30 min) on characteristics and anti-bacterial properties of synthesized AgNPs.

2. Materials and methods

2.1. Bacterial strain and cultivation

The strain *Bacillus subtilis* KMS2-2 used in this study was isolated from sediment samples of Uppanar estuary, Southeast coast of India and identified through conventional staining biochemical methods. For molecular identification, the strain was further characterized by 16 rDNA sequencing (Ruimy et al., 1994) in this study. For 16s rDNA sequencing, the genomic DNA was isolated and amplified by PCR with following primers: 27f (5′- AGAGTTTGATCCTGGCTCAG-3′) and 1492r (5′-TACGGTTACCTTGTTACGACTT-3′). The amplified DNA was sequenced at Xcelris Labs Limited (Ahmedabad, India) and sequences of 16s rDNA were compared against the GenBank database using standard nucleotide BLAST program. Further, the sequences of 16s rDNA were deposited to National Centre for Biotechnology Information (NCBI) and retrieved with an accession number as MN065454.1.

The bacterial strain *Bacillus subtilis* KMS2-2 was maintained in nutrient agar slant (Hi-Media, India) at 4 °C with periodical subculturing method and used as working culture preparation for AgNPs synthesis. The Gram negative (*Pseudomonas fluorescens* MTCC 1749, *Proteus mirabilis* MTCC 425 and *Escherichia coli* MTCC 1610) and Gram positive (*Bacillus cereus* and *Staphylococcus aureus* MTCC 2940) bacteria were previously procured from Microbial Type Culture Collection and Gene Bank (MTCC), Institute of Microbial Technology, Chandigarh, India and used to determine the inhibitory features of synthesized AgNPs.

2.2. Biomass production and AgNPs synthesis

The synthesis of AgNPs were done by the method of (Saravanan et al., 2018a) with slight modifications. The strain *Bacillus subtilis* KMS2-2 was grown in flask containing 500 ml of sterile Luria-Bertani broth (Hi-Media, India) for 48 h at room temperature with constant shaking at 100 rpm. After incubation, the grown culture was centrifuged (8000 rpm for 15 min) to collect the supernatant and remained biomass was discarded. Then, the collected supernatant was filtered using Whatman filter paper No. 42 (2.4 μm pore size) and used for extracellular synthesis of AgNPs. For AgNPs synthesis, the filtered supernatant was mixed with equal volume of previously prepared 1 mM Silver nitrate ($AgNO_3$) solution and incubated on rotating shaker (150 rpm) at room temperature for 72 h. With this above mixture, the positive (1 mM silver nitrate solution) and negative control (broth without inoculating bacteria) experiments were run parallel in this study. The reaction mixture was periodically checked for AgNPs synthesis by observing visible colour changes and using UV–vis spectrophotometer.

2.3. Collection, calcination and characterization of AgNPs

The synthesized AgNPs were collected from the reaction mixture by centrifugation at 8,000 rpm for 10 min. After collection, the nanoparticles were dried using hot air oven (100 °C for 12 h) and grinded to get powder form (crude). To study the effect of temperature on characteristics and anti-bacterial properties of AgNPs, the powdered particles were calcined at 200 °C for 30 min in muffle furnace. Further, the crude and calcined AgNPs were characterized by UV–vis spectrophotometer, Fourier Transformed Infrared (FT-IR), X-ray diffraction (XRD) and Scanning Electron Microscope coupled with Energy Dispersive X-ray spectroscopy (SEM-EDX) analysis. For UV analysis, the crude and calcined AgNPs were diluted with 2 ml double distilled water and subsequently measured in the range of 200–800 nm by UV–vis spectrophotometer. The presence of functional groups in crude and calcined AgNPs was determined using FT-IR (Spectrum RX I, Perkin Elmer, USA) ranging from 400 to 4000 cm^{-1} at a resolution of 4 cm^{-1}. The phase and crystal nature of AgNPs before and after calcination were studied by X-ray powder diffractometer (Phillips Xpert Pro, the Netherlands) running

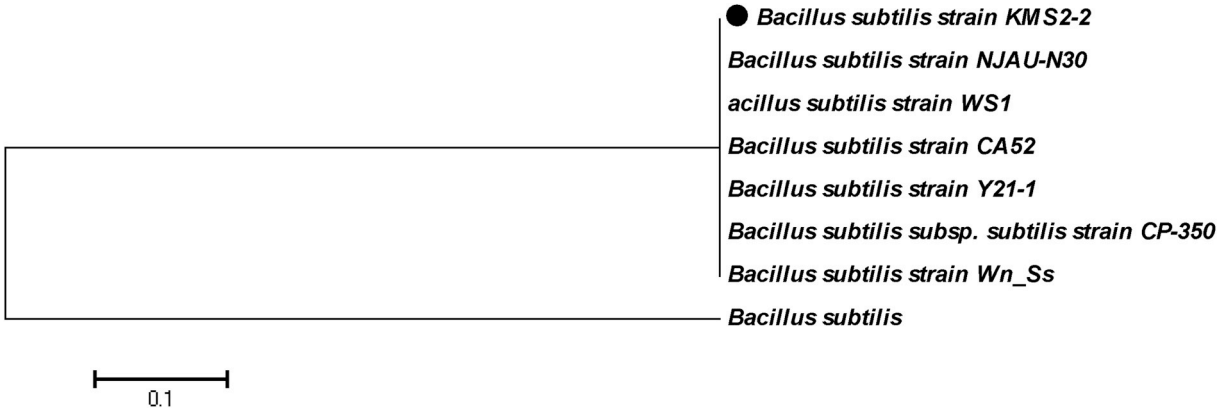

Fig. 1. Neighbour-joining tree, based upon 16S rDNA sequences of *B. subtilis* KMS2-2 and their closest relatives.

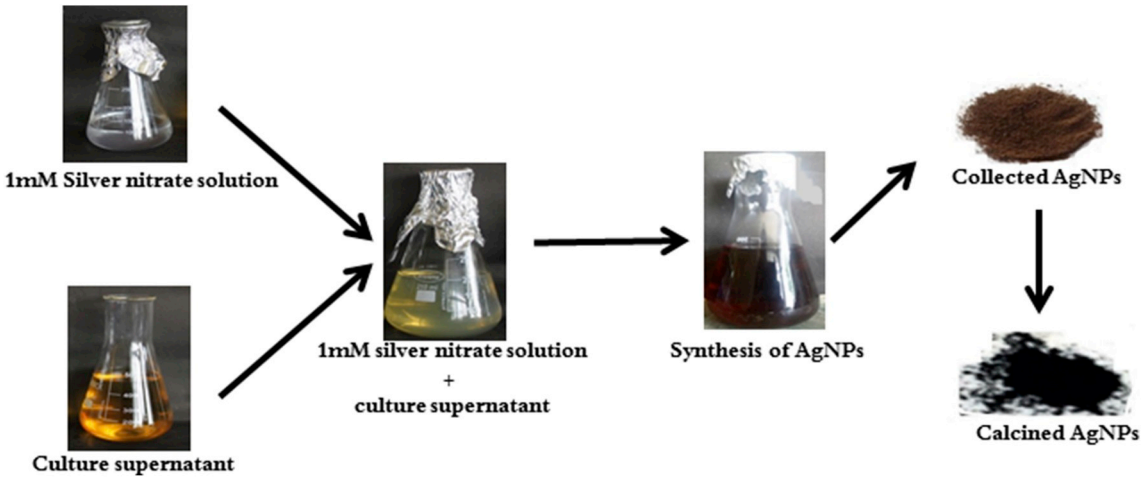

Fig. 2. shows the schematic representation of silver nanoparticles synthesized by *B.subtilis* KMS2-2.

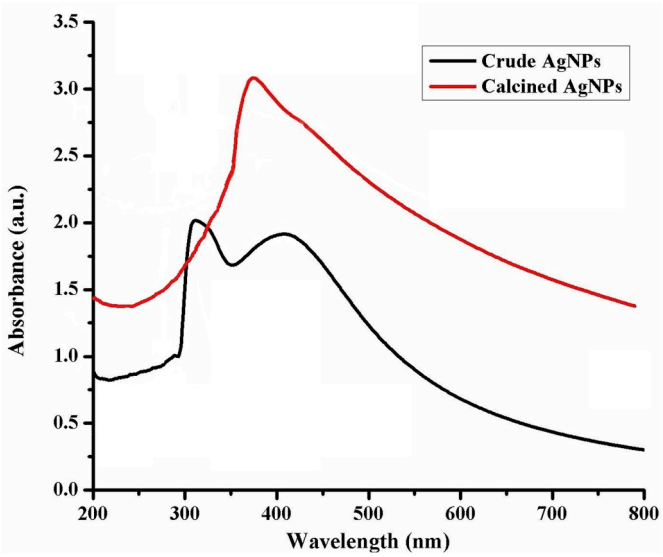

Fig. 3. UV–vis absorption spectra of crude and calcined AgNPs.

at 40 kV and 30 mA at 20-80 °C (2θ). Further, the morphology and elemental composition of AgNPs after and before calcination were studied by Scanning Electron Microscope (Carl Zeiss, Model EVO 18, Germany) coupled with Energy Dispersive X-ray spectroscopy (Oxford ISIS 300 EDS).

2.4. Anti-bacterial activity of crude and calcined AgNPs

The anti-bacterial activity of calcined AgNPs was studied by agar well diffusion method along with crude AgNPs (reaction mixture) against pathogenic bacteria such as, *Pseudomonas fluorescens* MTCC 1749, *Proteus mirabilis* MTCC 425, *Escherichia coli* MTCC 1610, *Bacillus cereus* and *Staphylococcus aureus* MTCC 2940. The stock solutions for calcined AgNPs were prepared at a final concentration of 0.5 mg/mL using distilled water as the solvent. For diffusion assay, the wells were made on Muller Hinton agar plates and swabbed with 12 h grown pathogenic bacterial broth cultures. Then, the different concentrations (25, 50, 75 and 100 µL) of crude and calcined AgNPs (100 µL) solution were loaded into each well and incubated at 37 °C for 24 h. The sensitivity of the tested bacteria was determined by measuring the diameter of the inhibition zone around each well (in mM).

3. Results and discussion

3.1. Identification of bacteria and AgNPs synthesis

The 16S rDNA sequencing results showed that bacterial strain used in this study had 99% identity with *Bacillus subtilis* when the sequence data subjected to nucleotide BLAST program (Fig. 1). The extra-cellular synthesis of AgNPs by *Bacillus subtilis* KMS2-2 was confirmed by the observing the colour changes in the reaction mixture from yellow into brown colour. The synthesis of AgNPs by *Bacillus subtilis* KMS2-2 is schematically represented in Fig. 2. In this study, the synthesis of AgNPs

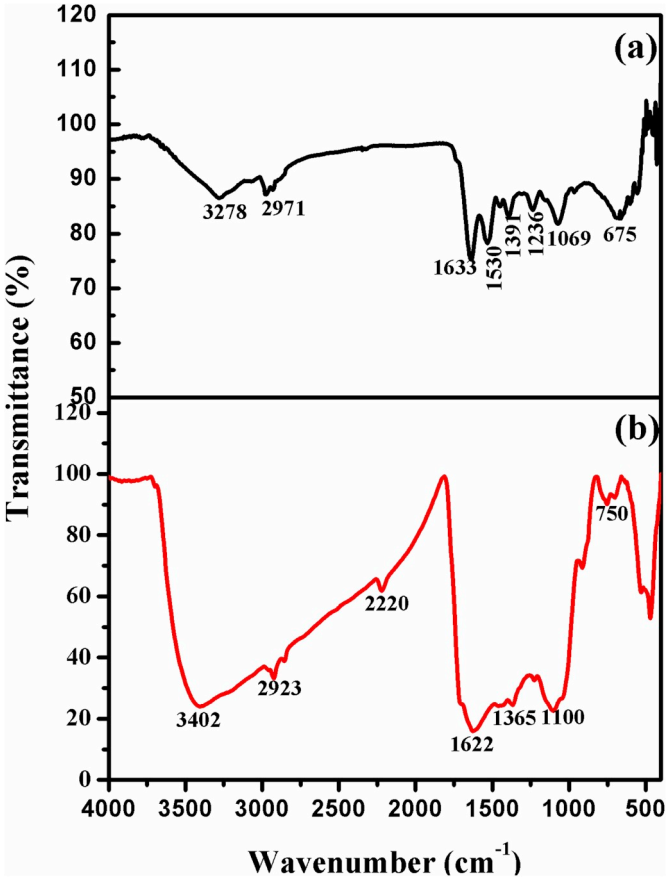

Fig. 4. IR absorption spectra of (a) crude and (b) calcined AgNPs.

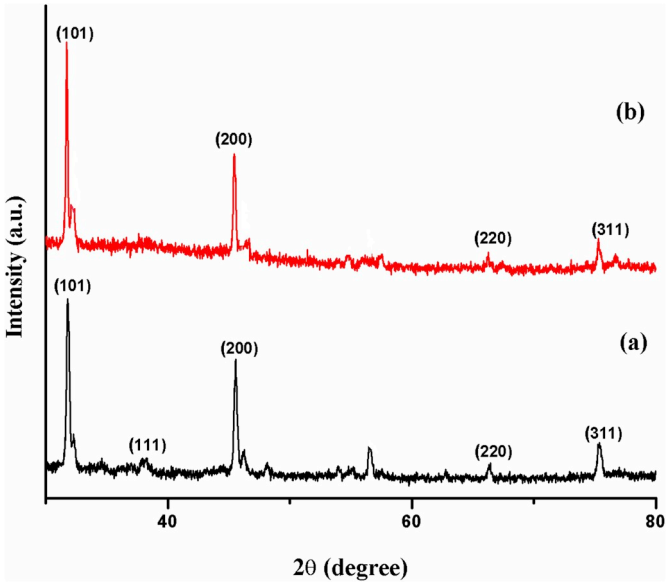

Fig. 5. XRD spectra of (a) crude and (b) calcined AgNPs.

was observed in the reaction mixture after 6 h contact time at room temperature. It has been previously reported that the biological synthesis of AgNPs mainly depends on many physical and chemical factors including temperature and reaction time etc. (Tippayawat et al., 2016).

3.2. Characterization of crude and calcined AgNPs

3.2.1. UV-spectral analysis of AgNPs

The UV–visible spectra of crude (reaction mixture) and calcined AgNPs are shown in Fig. 3. In the crude AgNPs spectrum, a strong Surface Plasmon Resonance (SPR) peak was observed at 420 which confirmed the reduction of Ag^{+} ions into AgNPs by biomolecules present in the supernatant. Likewise (Saravanan et al., 2018a), has also reported the characteristics (SPR) peak for AgNPs synthesized by *Bacillus brevis* (NCIM 2533) at 420 nm. Whereas, the SPR peak for AgNPs synthesized by plant extract of *Mentha piperita* was observed at 450 nm (MubarakAli et al., 2011). Generally, the characteristics peak for AgNPs can be noticed between 400-450 nm in the UV–Vis region (Samadi et al., 2010). The UV–vis spectrum of calcined AgNPs showed a strong SPR peak at 390 nm which indicated that calcination temperature altered the properties of nanoparticles. The changes in SPR peak position in the UV spectrum after calcination might be due to elimination of capping material from nanoparticles (Gharibshahi et al., 2017). Further, the calcination of nanoparticles with prolonged time period can increase the size and form the different types of crystal size (Tang et al., 2012). Kayani et al. (2015) reported that calcination temperature shifted (red shift) the absorption peak to larger wavelengths region for zinc oxide nanoparticles due to nanoparticles agglomeration.

3.2.2. FTIR analysis of AgNPs

The FTIR spectra of crude and calcined AgNPs are shown in Fig. 4a&b. IR spectrum of crude AgNPs show peaks at 3278, 2971, 1633, 1530, 1391, 1236, 1069 and 675 cm^{-1} (Fig. 4a). The strong adsorption peak at 3278 cm^{-1} corresponded to N–H functional groups of protein and O–H stretching vibration of alcohol and phenol (Monowar et al., 2018). The peak at 2971 cm^{-1} is due to C–H stretching of alkane. The band at 1633 and 1530 cm^{-1} corresponded to amide I and II containing carbonyl groups (C═O) (Singh et al., 2018). The peak at 1391 cm^{-1} attributed to the symmetric deformation of the CH_3 vibration, and the bands at 1236 cm^{-1} and 1069 cm^{-1} can be assigned to the C–O stretching vibrations of alcohols, carboxylic acid or C–N stretching of amines (Jyoti et al., 2016). Also, the peak at 675 cm^{-1} corresponded to -C═H bending of alkenes (Rajeshkumar and Malarkodi, 2014). From this spectrum analysis, major functional groups such as O–H, N–H, C–H, C═O and C–O groups containing biomolecules such as polysaccharides, protein and other components present in the culture supernatant might be responsible for reduction of Ag^{+} into AgNPs and these groups might have acted as capping/stabilization agent (Jyoti et al., 2016). IR spectra

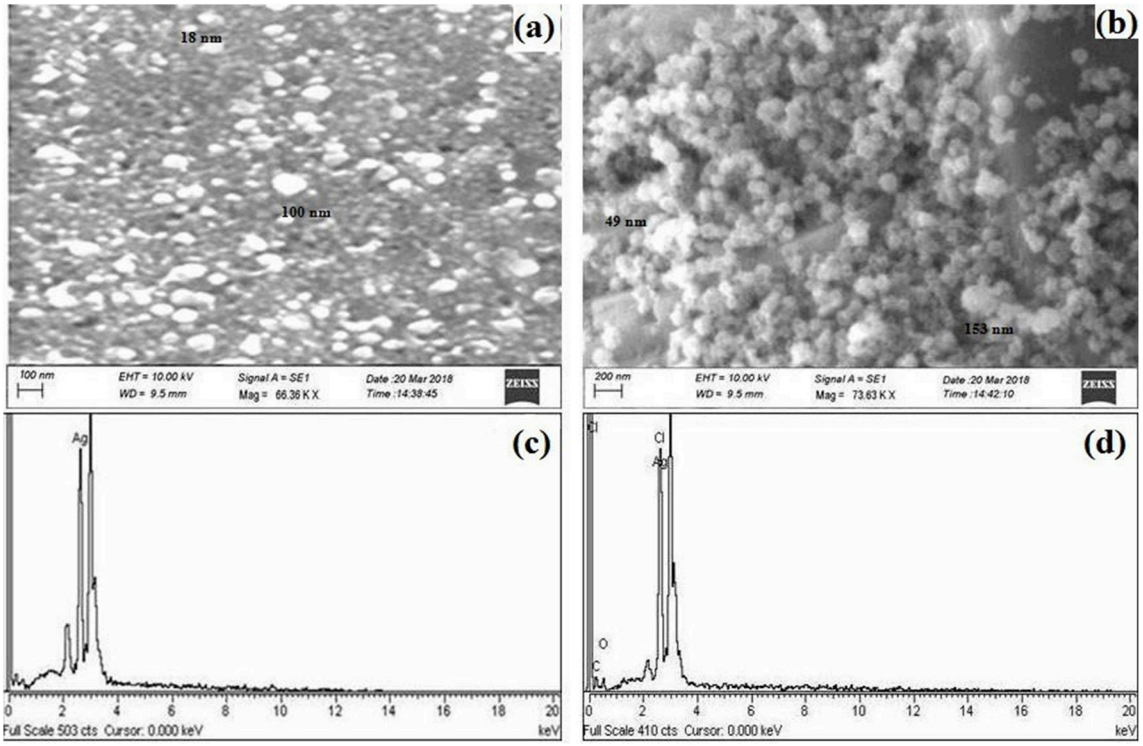

Fig. 6. SEM images of (a) crude AgNPs and (b) calcined AgNPs; EDX spectra of (c) crude AgNPs and (d) calcined AgNPs.

Table 1
Shows antibacterial activity of crude and calcined AgNPs.

Culture	Zone of Inhibition (mm)				
	Crude AgNPs				Calcined AgNPs
	10 µl	25 µl	50 µl	100 µl	100 µl
Pseudomonas fluorescens MTCC 1749	-	06	09	16	NZ
Proteus mirabilis MTCC 425	-	-	-	08	NZ
Escherichia coli MTCC 1610	-	08	10	13	NZ
Bacillus cereus	-	05	10	11	NZ
Staphylococcus aureus MTCC 2940	-	09	10	14	NZ

NZ: - No Zone of inhibition.

of AgNPs after calcination at 200 °C for 30 min are shown in (Fig. 4b). In the spectrum of calcined AgNPs, the adsorption peaks was observed at 3402, 2923, 2220, 1622, 1365, 1100 and 751 cm^{-1}. Some peaks not appear in IR spectrum of calcined AgNPs and this might be due to removal of peaks corresponding organic compounds by calcination at 200 °C. Gharibshahi et al. (2017) reported that the high purity of AgNPs could be obtained by increasing the calcination temperature.

3.2.3. X-ray diffraction analysis of AgNPs

Fig. 5a&b shows the typical XRD spectra of the AgNPs before and after calcination. The spectrum of crude AgNPs showed the diffraction peaks at 2θ values of 32.17°, 38.09°, 46.16°, 65.5° and 75.23° could be assigned the planes of (101), (111), (200), (220) and (311), respectively (Fig. 5a). Whereas, the diffraction peaks was observed for calcined AgNPs at 2θ values of 32.18°, 46.19°, 67.6° and 75.29° and could be assigned the plane of (101), (200), (220), and (311), respectively (Fig. 5b). The diffraction data obtained for crude and calcined AgNPs were compared with the powder diffraction data files of known compounds (ICDD/JCPDS, PDF Nos. 04–0783 and 84–0713). Results of X-ray diffraction analysis revealed that AgNPs before and after calcination was face-centered cubic, crystalline in nature and confirmed the presence of AgNPs formed by *Bacillus subtilis* KMS2-2. Goudarzi et al. (2016). stated that increasing the calcination temperature has resulted in an increase in crystalline size of AgNPs.

3.2.4. SEM-EDS analysis of AgNPs

SEM images were taken to analyze the structure, size and morphology of AgNPs after and before calcination. The SEM image of crude AgNPs showed the uniform spherical shaped particles and capped with biomolecules present in culture supernatant (Fig. 6a). Further, the particle size range between 18–100 nm was measured in the crude AgNPs. The spherical shaped structure with size range of 90 nm was observed for AgNPs synthesized by plant extract of *Mentha piperita* (MubarakAli et al., 2011). Also, Saravanan et al. (2018a) stated the AgNPs synthesized by *Phenerochaete chrysosporium* (MTCC-787) had different shapes, such as spherical and oval shapes with 34–90 nm in size range. However, the morphology and size of AgNPs varied after calcination and showed the uniform, spherical shaped structure with increase in size (Fig. 6b). The particles size was measured in the range of 49–153 nm after calcination. Previous studies has reported that the size of nanoparticles increased with increasing the calcination temperature (Shanaj and John, 2016; Singh et al., 2018). The EDX analysis showed the presence of elemental silver in the spectra of both crude and calcined AgNPs which is verified by the absorption peak at 2–3 KeV regions. These results indicating the reduction of Ag^{+} into Ag^{0} by biomolecules present in the bacterial supernatant.

3.3. Antibacterial activity of crude and calcined AgNPs

The antibacterial activities of crude and calcined AgNPs were tested against pathogenic bacteria such as *Pseudomonas fluorescens* MTCC 1749, *Proteus mirabilis* MTCC 425, *Escherichia coli* MTCC 1610, *Bacillus cereus* and *Staphylococcus aureus* MTCC 2940 by well diffusion method are shown in Table-1 and Fig. 7a–e. The highest inhibition zone of 16 mm was observed for crude AgNPs against *Pseudomonas fluorescens* MTCC 1749 (Fig. 7d), whereas; the lowest inhibition zone of 08 mm was noted against *Proteus mirabilis* MTCC 425 at 100 µL concentration (Fig. 7c). Results showed that the inhibitory activity of AgNPs increased with increases the reaction mixture (crude) volume. Maiti et al. (2014) stated that AgNPs synthesized by *Lycopersicon esculentum* extract did not show growth inhibitory activity at low concentration and showed good inhibitory activity when increases the concentration above 20µg/ml. The AgNPs synthesized by culture supernatant of *Streptacidiphilus durhamensis* are bacteriostatic at low concentration and bactericidal at high concentration (Buszewski et al., 2018). Previous studies suggested biologically synthesized AgNPs had potent antimicrobial, larvicidal and

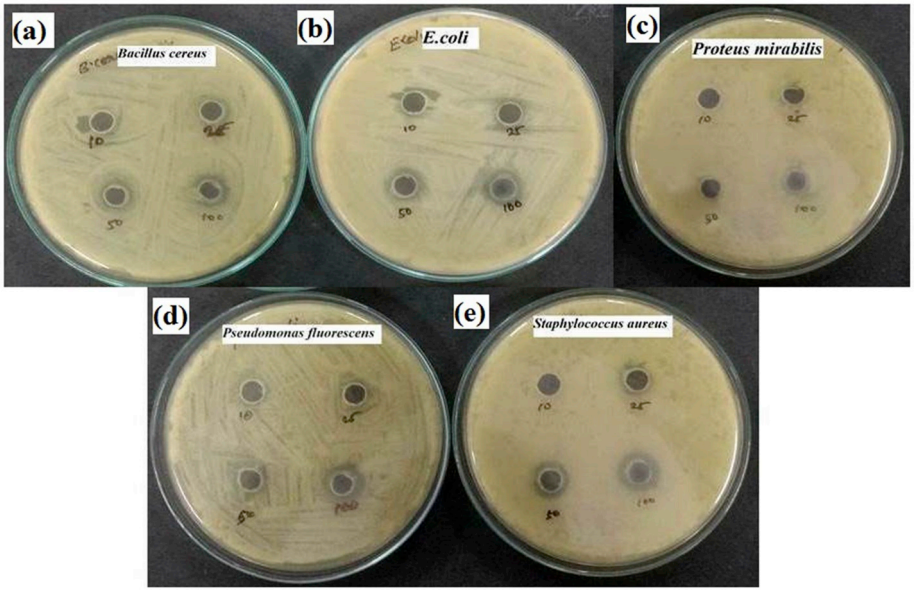

Fig. 7. Anti-bacterial activity of crude AgNPs (a) *Bacillus cereus* (b) *E.coli* (c) *Proteus mirabilis* (d) *Pseudomonas fluorescens* and (e) *Staphylococcus aureus*.

nematicidal activity (Mahmoud et al., 2016; Paul and Sinha, 2014; Shanmugasundaram and Balagurunathan, 2015). Further, the calcined AgNPs did not show the inhibitory activity in agar well diffusion method against tested bacterial strains. This observation revealed the bacterial inhibitory activity of AgNPs is decreased after calcination at 200 °C for 30 min. Sundrarajan et al. (2012) stated that the calcination temperature affects the antibacterial properties of nanoparticles and decrease the inhibitory activity with increasing the calcination temperature.

4. Conclusions

In this study, the AgNPs were extracellularly synthesized using culture supernatant of Gram positive bacterium *Bacillus subtilis* KMS2-2 and determined its inhibitory activity against pathogenic bacteria. In addition, the synthesized AgNPs were calcined at 200 °C for 30 min and characterized to study its effect in the morphology, size and antibacterial properties. Results showed that the crude AgNPs (reaction mixture) has good inhibitory activity against tested pathogens. However, the morphology, size and antibacterial characteristics of AgNPs changed after calcination. The calcined AgNPs did not show any inhibition for pathogenic bacteria at a tested concentration by well diffusion method in agar plates. Owning to such good inhibitory potent, the crude AgNPs can be used as an effective bacterial growth control in food packaging and biomedical fields. Follow-up studies involving the study on susceptibility of pathogenic bacteria in the presence of crude and calcined AgNPs by broth dilution method will be focused. Further, the inhibitory mechanisms of AgNPs against pathogenic bacteria will be studied in detail.

Acknowledgement

The authors thank to the authorities of Manonmaniam Sundaranar University, Tamil Nadu, India for providing the infrastructure facilities. DST-SERB, Govt. of India, National Post-Doctoral Fellowship grant (PDF/2015/000442) to K. Mathivanan is gratefully acknowledged.

Appendix A. Supplementary data

Supplementary data to this article can be found online at https://doi.org/10.1016/j.bcab.2019.101373.

References

Arya, A., Mishra, V., Chundawat, T.S., 2019. Green synthesis of silver nanoparticles from green algae (Botryococcus braunii) and its catalytic behavior for the synthesis of benzimidazoles. Chem. Data Collect. 20, 100190.

Banu, A.N., Balasubramanian, C., 2015. Extracellular synthesis of silver nanoparticles using Bacillus megaterium against malarial and dengue vector (Diptera: Culicidae). Parasitol. Res. 114, 4069–4079.

Boovaragamoorthy, G.M., Anbazhagan, M., Piruthiviraj, P., Pugazhendhi, A., Kumar, S. S., Al-Dhabi, N.A., Ghilan, A.-K.M., Arasu, M.V., Kaliannan, 2019. Clinically important microbial diversity and its antibiotic resistance pattern towards various drugs. J. Infect. Public Health. https://doi.org/10.1016/j.jiph.2019.08.008.

Buszewski, B., Railean-Plugaru, V., Pomastowski, P., Rafińska, K., Szultka-Mlynska, M., Golinska, P., Wypij, M., Laskowski, D., Dahm, H., 2018. Antimicrobial activity of biosilver nanoparticles produced by a novel *Streptacidiphilus durhamensis* strain. J. Microbiol. Immunol. Infect. 51, 45–54.

Deljou, A., Goudarzi, S., 2016. Green extracellular synthesis of the silver nanoparticles using thermophilic Bacillus sp. AZ1 and its antimicrobial activity against several human pathogenetic bacteria. Iran. J. Biotechnol. 14, 25.

Fathima, J.B., Pugazhendhi, A., Oves, M., Venis, R., 2018. Synthesis of eco-friendly copper nanoparticles for augmentation of catalytic degradation of organic dyes. J. Mol. Liq. 260, 1–8.

Gharibshahi, L., Saion, E., Gharibshahi, E., Shaari, A., Matori, K., 2017. Structural and optical properties of Ag nanoparticles synthesized by thermal treatment method. Mater 10, 402.

Goudarzi, M., Mir, N., Mousavi-Kamazani, M., Bagheri, S., Salavati-Niasari, M., 2016. Biosynthesis and characterization of silver nanoparticles prepared from two novel natural precursors by facile thermal decomposition methods. Sci. Rep. 6, 32539.

Hussein, H., Shaarawy, H., Hussien, N.H., Hawash, S., 2019. Preparation of nano-fertilizer blend from banana peels. Bull. Natl. Res. Cent. 43, 26.

Jacob, J.M., John, M.S., Jacob, A., Abitha, P., Kumar, S.S., Rajan, R., Natarajan, S., Pugazhendhi, A., 2018. Bactericidal coating of paper towels via sustainable biosynthesis of silver nanoparticles using Ocimum sanctum leaf extract. Mater. Res. Express. https://doi.org/10.1088/2053-1591/aafaed.

Jiang, Z., Shan, K., Song, J., Liu, J., Rajendran, S., Pugazhendhi, A., Jacob, J.A., Chen, B., 2019. Toxic effects of magnetic nanoparticles on normal cells and organs. Life Sci. 220, 156–161.

Jishma, P., Narayanan, R., Snigdha, S., Thomas, R., Radhakrishnan, E., 2018. Rapid degradative effect of microbially synthesized silver nanoparticles on textile dye in presence of sunlight. Biocatal. Agri. Biotechnol. 14, 410–417.

Jyoti, K., Baunthiyal, M., Singh, A., 2016. Characterization of silver nanoparticles synthesized using Urtica dioica Linn. leaves and their synergistic effects with antibiotics. J. Radiat. Res. Appl. Sci. 9, 217–227.

Kalimuthu, K., Babu, R.S., Venkataraman, D., Bilal, M., Gurunathan, S., 2008. Biosynthesis of silver nanocrystals by *Bacillus licheniformis*. Colloids Surfaces B Biointerfaces 65, 150–153.

Kathiravan, V., Ravi, S., Ashokkumar, S., 2014. Synthesis of silver nanoparticles from *Melia dubia* leaf extract and their in vitro anticancer activity. Spectrochim. Acta A Mol. Biomol. Spectrosc. 130, 116–121.

Kayani, Z.N., Saleemi, F., Batool, I., 2015. Effect of calcination temperature on the properties of ZnO nanoparticles. Appl. Phys. A 119, 713–720.

Kumar, G., Mathimani, T., Rene, E.R., Pugazhendhi, A., 2019. Application of nanotechnology in dark fermentation for enhanced biohydrogen production using inorganic nanoparticles. Int. J. Hydrogen Energy 44, 13106–13113.

Kumar, P.S.M., Ponnusamy, V.K., Deepthi, K.R., Kumar, G., Pugazhendhi, A.,H., Thiripuranthagan, S., Pal, U., Krishnan, S., 2018. Controlled synthesis of Pt nanoparticle supported TiO_2 nanorods as efficient and stable electrocatalysts for the oxygen reduction reaction. J. Mater. Chem. 6, 23435–23444.

Mahmoud, W.M., Abdelmoneim, T.S., Elazzazy, A.M., 2016. The impact of silver nanoparticles produced by Bacillus pumilus as antimicrobial and nematicide. Front. Microbiol. 7, 1746.

Maiti, S., Krishnan, D., Barman, G., Ghosh, S.K., Laha, J.K., 2014. Antimicrobial activities of silver nanoparticles synthesized from *Lycopersicon esculentum* extract. J. Anal. Sci. Technol. 5, 40.

Monowar, T., Rahman, M., Bhore, S., Raju, G., Sathasivam, K., 2018. Silver nanoparticles synthesized by using the endophytic bacterium *Pantoea ananatis* are promising antimicrobial agents against multidrug resistant bacteria. Mol 23, 3220.

MubarakAli, D., Thajuddin, N., Jeganathan, K., Gunasekaran, M., 2011. Plant extract mediated synthesis of silver and gold nanoparticles and its antibacterial activity against clinically isolated pathogens. Colloids Surfaces B Biointerfaces 85, 360–365.

Munteanu, A., Florescu, I., Nitescu, C., 2016. A modern method of treatment: the role of silver dressings in promoting healing and preventing pathological scarring in patients with burn wounds. J. Med. Life 9, 306.

Murphin Kumar, P.S., Thiripuranthagan, S., Imai, T., Kumar, G., Pugazhendhi, A., Vijayan, S.R., Esparza, R., Abe, H., Krishnan, S., 2017. Pt nanoparticles supported on mesoporous CeO2 nanostructures obtained through green approach for efficient catalytic performance toward ethanol electro-oxidation. ACS Sustain. Chem. Eng. 5, 11290–11299.

Oves, M., Aslam, M., Rauf, M.A., Qayyum, S., Qari, H.A., Khan, M.S., Alam, M.Z., Tabrez, S., Pugazhendhi, A., Ismail, I., 2018. Antimicrobial and anticancer activities of silver nanoparticles synthesized from the root hair extract of Phoenix dactylifera. Mater. Sci. Eng. C Mater. Biol. Appl. 89, 429–443.

Patra, J.K., Baek, K.-H., 2014. Green nanobiotechnology: factors affecting synthesis and characterization techniques. J. Nanomater. 2014, 219.

Paul, D., Sinha, S.N., 2014. Extracellular synthesis of silver nanoparticles using Pseudomonas aeruginosa KUPSB12 and its antibacterial activity. Jordan J. Biol. Sci. 147, 1–6.

Premkumar, J., Sudhakar, T., Dhakal, A., Shrestha, J.B., Krishnakumar, S., Balashanmugam, P., 2018. Synthesis of silver nanoparticles (AgNPs) from cinnamon against bacterial pathogens. Biocatal. Agric. Biotechnol. 15, 311–316.

Pugazhendhi, A., Edison, T.N.J.I., Karuppusamy, I., Kathirvel, B., 2018. Inorganic nanoparticles: a potential cancer therapy for human welfare. Int. J. Pharm. 539, 104–111.

Pugazhendhi, A., Kumar, S.S., Manikandan, M., Saravanan, M.J.M.p., 2018. Photocatalytic properties and antimicrobial efficacy of Fe doped CuO nanoparticles against the pathogenic bacteria and fungi. Microb. Pathog. 122, 84–89.

Pugazhendhi, A., Prabakar, D., Jacob, J.M., Karuppusamy, I., Saratale, R.G., 2018. Synthesis and characterization of silver nanoparticles using *Gelidium amansii* and its antimicrobial property against various pathogenic bacteria. Microb. Pathog. 114, 41–45.

Pugazhendhi, A., Prabhu, R., Muruganantham, K., Shanmuganathan, R., Natarajan, S.J.J. o.P., Biology, P.B., 2019. Anticancer, antimicrobial and photocatalytic activities of green synthesized magnesium oxide nanoparticles (MgONPs) using aqueous extract of *Sargassum wightii*. J. Photochem. Photobiol. B Biol. 190, 86–97.

Pugazhendhi, A., Shobana, S., Nguyen, D.D., Banu, J.R., Sivagurunathan, P., Chang, S. W., Ponnusamy, V.K., Kumar, G., 2018. Application of nanotechnology (nanoparticles) in dark fermentative hydrogen production. Int. J. Hydrogen Energy 44, 1431–1440.

Rajeshkumar, S., Malarkodi, C., 2014. In vitro antibacterial activity and mechanism of silver nanoparticles against foodborne pathogens. Bioinorgan. Chem. Appl. 2014.

Ramkumar, V.S., Pugazhendhi, A., Gopalakrishnan, K., Sivagurunathan, P., Saratale, G. D., Dung, T.N.B., Kannapiran, E.J.B.r., 2017. Biofabrication and characterization of silver nanoparticles using aqueous extract of seaweed Enteromorpha compressa and its biomedical properties. Biotechnol. Rep. 14, 1–7.

Ruimy, R., Breittmayer, V., Elbaze, P., Lafay, B., Boussemart, O., Gauthier, M., Christen, R., 1994. Phylogenetic analysis and assessment of the genera Vibrio, Photobacterium, Aeromonas, and Plesiomonas deduced from small-subunit rRNA sequences. Int. J. Syst. Evol. Microbiol. 44, 416–426.

Samadi, N., Hosseini, S., Fazeli, A., Fazeli, M., 2010. Synthesis and antimicrobial effects of silver nanoparticles produced by chemical reduction method. Daru 18, 168.
Saratale, G.D., Saratale, R.G., Benelli, G., Kumar, G., Pugazhendhi, A., Kim, D.-S., Shin, H.-S., 2017. Anti-diabetic potential of silver nanoparticles synthesized with Argyreia nervosa leaf extract high synergistic antibacterial activity with standard antibiotics against foodborne bacteria. J. Clust. Sci. 28, 1709–1727.
Saratale, R.G., Karuppusamy, I., Saratale, G.D., Pugazhendhi, A., Kumar, G., Park, Y., Ghodake, G.S., Bharagava, R.N., Banu, J.R., Shin, H.S., 2018. A comprehensive review on green nanomaterials using biological systems: recent perception and their future applications. Colloids Surfaces B Biointerfaces 170, 20–35.
Saratale, R.G., Saratale, G.D., Shin, H.S., Jacob, J.M., Pugazhendhi, A., Bhaisare, M., Kumar, G., 2018. New insights on the green synthesis of metallic nanoparticles using plant and waste biomaterials: current knowledge, their agricultural and environmental applications. Environ. Sci. Pollut. Control Ser. 25, 10164–10183.
Saravanan, M., Arokiyaraj, S., Lakshmi, T., Pugazhendhi, A., 2018. Synthesis of silver nanoparticles from Phenerochaete chrysosporium (MTCC-787) and their antibacterial activity against human pathogenic bacteria. Microb. Pathog. 117, 68–72.
Saravanan, M., Barik, S.K., MubarakAli, D., Prakash, P., Pugazhendhi, A., 2018. Synthesis of silver nanoparticles from *Bacillus brevis* (NCIM 2533) and their antibacterial activity against pathogenic bacteria. Microb. Pathog. 116, 221–226.
Saravanan, M., Niguse, S., Abdulkader, M., Tsegay, E., Hailekiros, H., Gebrekidan, A., Araya, T., Pugazhendhi, A., 2018. Review on emergence of drug-resistant tuberculosis (MDR & XDR-TB) and its molecular diagnosis in Ethiopia. Microb. Pathog. 117, 237–242.
Sathiyavimal, S., Vasantharaj, S., Bharathi, D., Saravanan, M., Manikandan, E., Kumar, S. S., Pugazhendhi, A., 2018. Biogenesis of copper oxide nanoparticles (CuONPs) using Sida acuta and their incorporation over cotton fabrics to prevent the pathogenicity of Gram negative and Gram positive bacteria. J. Photochem. Photobiol. B Biol. 188, 126–134.
Shanaj, B., John, X., 2016. Effect of calcination time on structural, optical and antimicrobial properties of nickel oxide nanoparticles. J. Theor. Comput. Sci 3.
Shanmuganathan, R., Karuppusamy, I., Saravanan, M., Muthukumar, H., Ponnuchamy, K., Ramkumar, V.S., Pugazhendhi, A., 2019. Synthesis of Silver nanoparticles and their biomedical applications-A comprehensive review. Curr. Pharmaceut. Des. https://doi.org/10.2174/1381612825666190708185506.
Shanmuganathan, R., MubarakAli, D., Prabakar, D., Muthukumar, H., Thajuddin, N., Kumar, S.S., Pugazhendhi, A., 2018. An enhancement of antimicrobial efficacy of biogenic and ceftriaxone-conjugated silver nanoparticles: green approach. Environ. Sci. Pollut. Res. Int. 25, 10362–10370.
Shanmugasundaram, T., Balagurunathan, R., 2015. Mosquito larvicidal activity of silver nanoparticles synthesised using actinobacterium, Streptomyces sp. M25 against Anopheles subpictus, Culex quinquefasciatus and Aedes aegypti. J. Parasit. Dis. 39, 677–684.
Singh, H., Du, J., Singh, P., Yi, T.H., 2018. Extracellular synthesis of silver nanoparticles by *Pseudomonas* sp. THG-LS1. 4 and their antimicrobial application. J. Pharm. Anal. 8, 258–264.
Soliman, H., Elsayed, A., Dyaa, A., 2018. Antimicrobial activity of silver nanoparticles biosynthesised by *Rhodotorula* sp. strain ATL72. Egypt. J. Basic Appl. Sci. 5, 228–233.
Sundrarajan, M., Suresh, J., Gandhi, R.R., 2012. A comparative study on antibacterial properties of MgO nanoparticles prepared under different calcination temperature. Digest J. Nanomater. Biostructures 7, 983–989.
Tang, Z.-X., Fang, X.-J., Zhang, Z.-L., Zhou, T., Zhang, X.-Y., Shi, L.-E., 2012. Nanosize MgO as antibacterial agent: preparation and characteristics. Braz. J. Chem. Eng. 29, 775–781.
Thomas, R., Janardhanan, A., Varghese, R.T., Soniya, E., Mathew, J., Radhakrishnan, E., 2014. Antibacterial properties of silver nanoparticles synthesized by marine Ochrobactrum sp. Braz. J. Microbiol. 45, 1221–1227.
Tippayawat, P., Phromviyo, N., Boueroy, P., Chompoosor, A., 2016. Green synthesis of silver nanoparticles in aloe vera plant extract prepared by a hydrothermal method and their synergistic antibacterial activity. PeerJ 4, e2589.
Van Duin, D., Paterson, D.L., 2016. Multidrug-resistant bacteria in the community: trends and lessons learned. Infect. Dis. Clin. 30, 377–390.
Vasantharaj, S., Sathiyavimal, S., Senthilkumar, P., LewisOscar, F., Pugazhendhi, A.J.J.o. P., Biology, P.B., 2019. Biosynthesis of iron oxide nanoparticles using leaf extract of Ruellia tuberosa: antimicrobial properties and their applications in photocatalytic degradation. J. Photochem. Photobiol. B Biol. 192, 74–82.
Wong, K.K., Cheung, S.O., Huang, L., Niu, J., Tao, C., Ho, C.M., Che, C.M., Tam, P.K., 2009. Further evidence of the anti-inflammatory effects of silver nanoparticles. ChemMedChem: Chem. Enabling Drug Discov. 4, 1129–1135.